Role of Focal Adhesions and Mechanical Stresses in the Formation and Progression of the Lamellum Interface

Tom Shemesh,[†] Alexander B. Verkhovsky,[‡] Tatyana M. Svitkina,[§] Alexander D. Bershadsky,[¶] and Michael M. Kozlov[†*]

[†]Department of Physiology and Pharmacology, Sackler Faculty of Medicine, Tel Aviv University, 69978 Tel Aviv, Israel; [‡]Laboratory of Cell Biophysics, Ecole Polytechnique Fédérale de Lausanne, Lausanne, Switzerland; [§]Department of Biology, University of Pennsylvania, Philadelphia, Pennsylvania; and [¶]Department of Molecular Cell Biology, The Weizmann Institute of Science, 76100 Rehovot, Israel

ABSTRACT Actin network in the front part of a moving cell is organized into a lamellipodium and a lamellum. A distinct lamellipodium-lamellum interface is associated with focal adhesions and consists of a series of arclike segments linking neighboring focal adhesions in the front row. The interface advances by leaping onto new rows of focal adhesions maturating underneath the lamellipodium. We propose a mechanism of the lamellipodium-lamellum boundary generation, shape formation, and progression based on the elastic stresses generated in the lamellipodial actin gel by its friction against the focal adhesions. The crucial assumption of the model is that stretching stresses trigger actin gel disintegration. We compute the stress distribution throughout the actin gel and show that the gel-disintegrating stresses drive formation of a gel boundary passing through the row of focal adhesions. Our computations recover the lamellipodium-lamellum boundary shapes detected in cells and predict the mode of the boundary transition to the row of the newly maturing focal adhesions in agreement with the experimental observations. The model fully accounts for the current phenomenology of the lamellipodium-lamellum interface formation and advancing, and makes experimentally testable predictions on the dependence of these phenomena on the sizes of the focal adhesions, the character of the focal adhesion distribution on the substrate, and the velocity of the actin retrograde flow with respect to the focal adhesions. The phase diagram resulting from the model provides a background for quantitative classification of different cell types with respect to their ability to form a lamellipodium-lamellum interface. In addition, the model suggests a mechanism of nucleation of the dorsal and arclike actin bundles found in the lamellum.

INTRODUCTION

Lamellipodium-lamellum interface

The ability of cells to move on extracellular matrices and substrates is due to two major factors: the actin-based machinery generating intracellular forces, and protein complexes called focal adhesions (FAs) mediating transmission of these forces to extracellular substrates (1–4). Although being of critical importance for cell motility, the cross talk between the intracellular actin system and the focal adhesion complexes is poorly understood. Here we propose a physical mechanism by which the interaction between the actin filaments and the FAs determines formation and progression of the lamellipodium-lamellum interface which is of a primary importance for understanding the mechanism of cell motility.

The complex system of actin filaments spanning the volume of a moving cell can be subdivided into distinct zones differing in their dynamic behavior, structure, and function. These zones are ordered in space sequentially beginning from the cell leading edge toward the cell interior (5). The first two zones are the lamellipodium, which underlies the cell membrane at the leading edge, and the lamellum adjacent to the lamellipodium and propagating further into the cell volume (6). In spite of their proximity, the lamellipodium and lamellum appear to represent two largely independent actin domains (7). The lamellipodium actin is assembled into a homogeneous gel of branched and cross-linked filaments undergoing polymerization next to the interface with the leading edge membrane (7–9). This actin gel moves from the leading edge toward the cell center in so-called retrograde flow (10–12). The characteristic velocities of this movement determined with respect to the leading edge membrane vary for different cell types between few hundreds of nanometers to several microns per minute (7,13). Branched actin filaments in the lamellipodium are nucleated by the Arp2/3 complex and their polymerization is regulated by a bunch of accessory proteins (14,15). It has been established that polymerization of the lamellipodium actin generates a mechanical force pushing the leading edge membrane forward (3,4,16,17).

The lamellum actin also moves in the retrograde direction, but the rate of this movement is several times slower than in the lamellipodium (7,13). Most of the lamellum actin is organized into bundles with a sparser network of actin filaments as well as other cytoskeletal fibrils between them (18,19). In contrast to the lamellipodium, Arp2/3 is absent from the lamellum so that the actin bundle formation and polymerization must be driven by other mechanisms and involve other proteins. The forces within lamellum depend mainly on myosin-IIA activity, which is responsible for both cell traction force generation and retrograde F-actin flow (20).

Submitted April 7, 2009, and accepted for publication May 15, 2009.

*Correspondence: michk@post.tau.ac.il

Editor: Alexander Mogilner.

0006-3495/09/09/1254/11 $2.00

doi: 10.1016/j.bpj.2009.05.065

The lamellipodium and lamellum actin networks are separated by a distinct interface, which is marked by an abrupt change of the velocity of the retrograde actin flow and a sharp change of the actin network density and structure (7,8,13). This distinction is especially clear for relatively slowly moving fibroblasts and epithelial cells (7,8,13). Revealing the physical forces responsible for the generation and dynamics of the lamellipodium-lamellum interface is of a primary importance for understanding the factors governing organization of actin at the cell front into the spatially segregated and essentially distinct domains.

According to the recent observations, both position and movement of the lamellipodium-lamellum interface are related to the focal adhesions. The mature micron-sized FAs were not observed in the lamellipodium per se but, essentially, they colocalized with the lamellipodium-lamellum interface (7,13). In spreading and moving fibroblasts and B16 melanoma cells, the lamellipodium-lamellum interface has a wave-like shape consisting of distinct arcs bulging toward the cell interior, with FAs in the arc intercepts (Fig. 1). Notably, the same FAs are associated with the distal tips of filament bundles stretching into the lamellum.

In the course of cell movement, the lamellipodium-lamellum interface follows the advancing leading edge. The intermediate steps of this process consist in formation of nascent FAs between the lamellipodium-lamellum interface and the leading edge, growth of these adhesions, and, finally, transition of the lamellipodium-lamellar interface to the row of the newly matured focal adhesions (13). A crucial role of FAs in the lamellipodium-lamellum interface formation was confirmed by the observations that, in the absence of the focal adhesions (as in the case of cells spread on polylysine-coated substrates), the lamellipodium-lamellum interface did not emerge (13). Moreover, it was recently shown that downregulation of talin, which is necessary for FA formation, prevents formation of the lamellipodium-lamellum interface (21).

Main hypothesis and the qualitative essence of the proposed model for the lamellipodium-lamellum interface formation and dynamics

Based on the above phenomenological data, we suggest that the force driving the generation of the lamellipodium-lamellum interface comes from the interaction between the moving actin gel and the immobile focal adhesions. We consider the lamellipodium actin network as an elastic medium (22), which slides toward the cell center over a row of FAs. It was recently established that the retrograde actin flow in lamellipodia and lamella brushes against the immobile focal adhesions, which results in friction forces between actin and the FAs (23,24). We consider here how such friction generates the lamellipodium-lamellum interface.

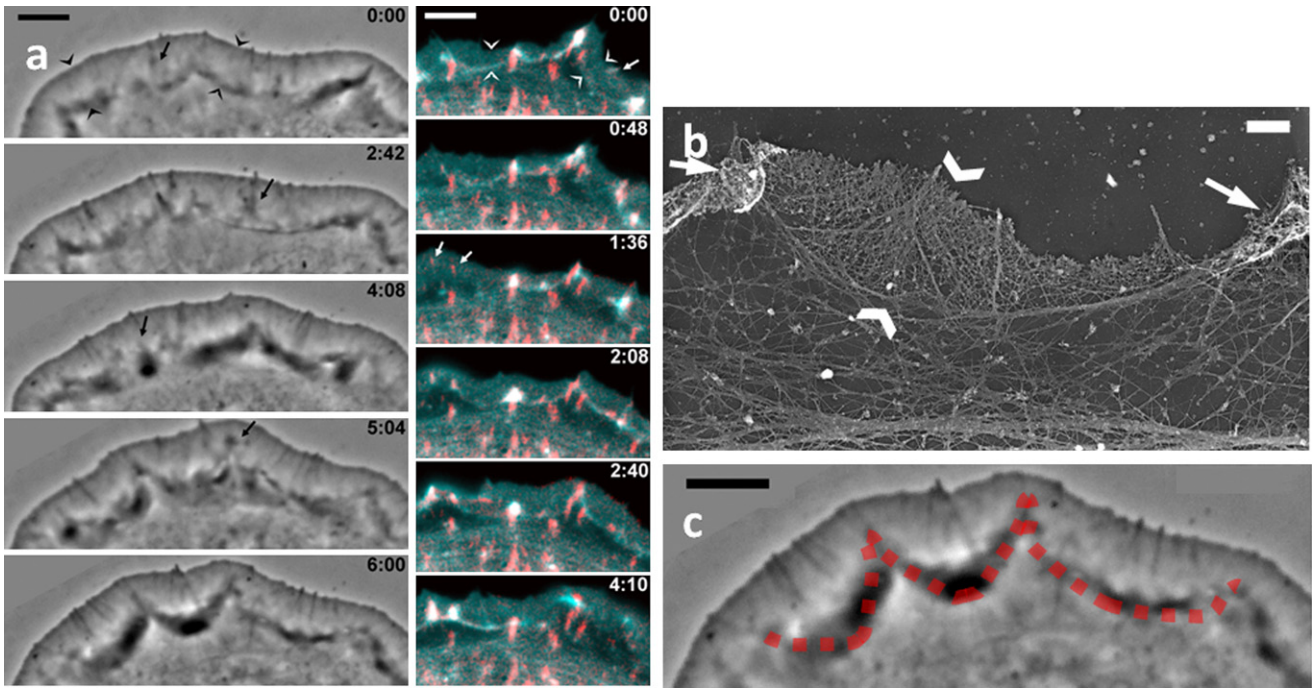

FIGURE 1 (*a*) Spreading Swiss 3T3 fibroblast (*left panel*, phase contrast) and REF-52 fibroblast (*right panel*, paxillin labeling of the focal adhesions is shown in *red*, phalloidin actin labeling in *cyan*, and overlap of both appears *white*). Arrowheads show the limits of the lamellipodium; arrows show the nascent adhesions within the lamellipodium; and time is indicated in min. Scale bar, 5 μm. (*b*) *Xenopus* fibroblast (platinum replica electron microscopy). Arrowheads show the limits of the lamellipodium; arrows, the adhesions. Scale bar, 1 μm. (*c*) Fitting of the model prediction to the observed shape of the lamellipodium-lamellum interface (*red dashed lines*).

The calculations below show that the FA-actin interaction produces strains and stresses within the actin gel, which are distributed over the gel in such a way that the gel regions between the FAs are stretched. Our main assumption is that when the stretching stress exceeds some threshold value, σ_{th}, it leads to instantaneous (in the relevant timescale) disintegration of the actin network. Similar assumption of the actin gel rupture under tensile stress was proposed for understanding the gel symmetry breaking in the course of formation of actin comet tails, which drive intracellular propulsion of internalized bacteria such as *Listeria monocytogenes* and in vitro movement of microspheres simulating actin polymerization-dependent motility of cellular organelles (25,26). Generally, the stress-driven disassembly of actin filaments must be due to mechano-chemical coupling (25). Here we suggest that the stretching stresses drastically accelerate a specific process of severing of actin filaments by specialized proteins such as the ADF/cofilin family proteins (27–32). We propose that this stretching-enhanced severing of the actin network is responsible for localized disassembly of >90% of the F-actin generated at the cell leading edge (7,8), which results in formation of the lamellipodium-lamellum interface. We show that the generated interface passes through the row of the FAs and has a shape of a chain of arcs similar to that observed within cells.

We further address movement of the lamellipodium-lamellum interface to the row of the newly maturating focal adhesions. To this end, we consider the changes of the stress distribution and the related disintegration of the lamellipodium actin network accompanying the growth of the new FAs underneath the actin gel between the existing lamellipodium-lamellum interface and the cell leading edge.

The model we suggest accounts for the whole set of the phenomenological data on the formation and progression of the lamellipodium-lamellum interface. It provides experimentally testable predictions about the character of the lamellipodium-lamellum interface for different dimensions of the focal adhesions and distances between them, and for different rates of the actin motion with respect to the focal adhesions. The quantitative predictions of the model are presented as a phase diagram, which can serve for classification of different cell states and types according to their ability to form the lamellipodium-lamellum interface. The model also allows for speculations about the nucleation of actin bundles in the lamellum downstream of the lamellipodium-lamellum interface.

MODEL

Actin gel and focal adhesions

We model the lamellipodium actin network as a purely elastic gel of actin filaments (22), which is bound on one side by the leading edge membrane (Fig. 2). The gel undergoes polymerization against the membrane, which

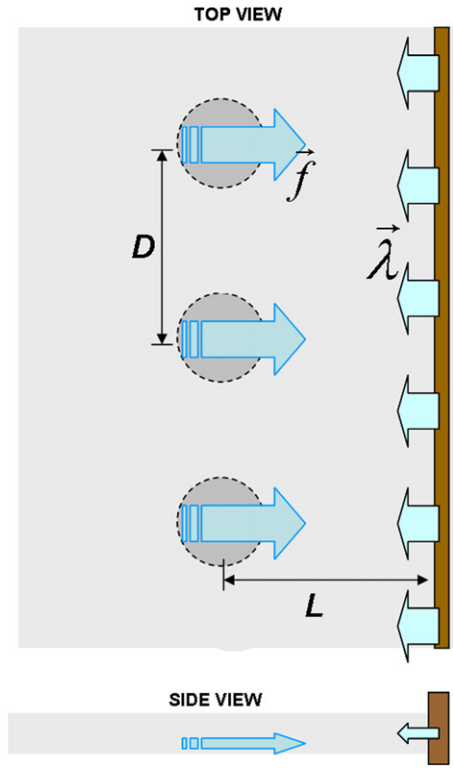

FIGURE 2 Schematic presentations of the system model and the notations.

generates a force pushing the gel from the membrane toward the cell center and resulting in the retrograde actin movement. Although, in general, the cell leading edge may crawl with respect to the substrate, we assume in the main analysis that the rate of this crawling is much smaller than that of the retrograde movement of the actin gel, which is true for most cells, except, perhaps, for keratocytes (15,33). Hence, we neglect the leading edge movement, and take the velocity of the actin retrograde flow to be $v_{retro} = 5\mu m/min$ (13). The effects of the leading edge movement and, specifically, the case of fast-crawling keratocytes are discussed in Predictions and Implications, below. Based on the observations in Alexandrova et al. (13), we will also neglect, for simplicity, the possible deformations of the leading edge and assume it to be represented by a straight line.

We consider the focal adhesions as circular discrete areas that are located between the gel and the substrate and immobilized on the substrate. It was shown in several recent experimental studies that the newly formed (i.e., nascent) focal adhesions form mainly underneath the lamellipodium (13,34). Whereas the mechanism of this process has not been well understood, a plausible model suggested in Choi et al. (34) assumes that the FA generation is mediated by association of ligated integrins or their nanoclusters with polymerizing actin network. According to this model the integrin-actin association is a slow process taking 10–20 s, which explains the existence of a micron-sized spatial gap between the lamellipodium edge and the focal adhesions.

Furthermore, formation and stabilization of a focal adhesion must be a relatively rare event that results in significant separations between the FAs. According to the observations (13), we assume that the FAs are ordered in a row parallel to the leading edge (Fig. 2).

The FAs exerts friction forces to the gel which are directed oppositely to the actin velocity, i.e., toward the leading edge membrane. This generates stresses in the gel, which are characterized by distribution of the maximal local stress σ_1 (see the Supporting Material A for rigorous definitions). We propose that in the regions, where the maximal stress σ_1 exceeds a positive (corresponding to stretching) threshold value σ_{th}, the gel disintegrates. The stretching stresses larger than the threshold value, $\sigma > \sigma_{th}$, will be referred to as the gel-disintegrating stresses.

Concerning the dynamic characteristics of the system, we make the following assumptions. The development of mechanical stresses within the gel is instantaneous, meaning that the gel is described as an elastic medium (22). Provided that the gel-disintegrating stresses are built up within the system, the gel disassembly begins after a characteristic time τ_{rup} needed for generation of an initial rupture. The following process of the gel disassembly is instantaneous compared to τ_{rup}, meaning that the latter determines the overall rate of the gel disintegration. Support for this assumption comes from examination of phase-contrast movies of the oscillations of the lamellipodium-lamellum interface (see Movie S1 in the Supporting Material). We propose that these oscillations result from a periodic disintegration and restoration of a stretched region of the actin gel next to the lamellipodium-lamellum interface. The observed oscillation period is used for setting the rupture time in our model, $\tau_{rup} = 11$ s.

The relevant geometrical parameters of the system are the radius of a mature focal adhesion, R_{FA}, the distance L between the FA row and the membrane edge, and the spacing D between the FA centers. The physical parameters are the friction force f between the gel and the focal adhesions related to the FA unit area, and the threshold stress σ_{th}. The parameter $\sigma_{th} = 40$ Pa is found below from fitting the calculated shapes of the emerging gel boundaries to the observed shapes of the lamellipodium-lamellum interface. We will explore the ranges of other parameters around the realistic values of $R_{FA} = 0.6$ μm, $L = 4$ μm, $D = 5$ μm (13), and $f = 500$ Pa, the latter corresponding to the experimentally feasible average force of ~100pN/μm acting on the gel from the leading edge membrane (3,4) and balanced by the total friction force.

Outline and methods of the analysis

Our first aim is to find the conditions for generation of the gel boundary by a single row of focal adhesions and to determine the boundary shape. To this end, we compute the distribution of stresses in a semiinfinite actin gel bound on one side by the leading edge membrane; we find the region of the gel-disintegrating stress. We seek for conditions where this region spans the entire distance between the neighboring focal adhesions. We assume that the gel collapses in this region, hence, creating a break in the initially continuous actin network and forming a free boundary representing the lamellipodium-lamellum interface. We compute the equilibrium shape of the emerging boundary and reveal its steady-state dynamics. We analyze quantitatively the parameter ranges allowing for formation of the lamellipodium-lamellum interface and present the results in the form of a phase diagram.

Our second goal is to analyze the transition of the gel boundary to a row of newly maturating focal adhesions. Based on the results obtained for one FA row, we consider the change of the stress distribution within the gel generated by the new FA row, and analyze the related disintegration of the actin network.

Computations of the elastic stresses within the gel are performed by the standard methods of the continuum theory of elasticity (see Supporting Material A) under the following boundary conditions. At the free gel boundary generated as a result of the gel disintegration, the component of the stress normal to the boundary must vanish. Along the gel areas right above the focal adhesions, the force pushing the gel toward the membrane and related to the unit area of FAs has a given value f. At the interface between the actin gel and the leading edge membrane, the total force Λ acting on the gel from the membrane equals the total force applied by the focal adhesions.

To take into account the gradual polymerization of the actin gel, the stress computation is performed repeatedly after infinitesimal time steps determining incremental insertions of new gel elements at the gel-membrane interface. This corresponds to infinitesimal shifts of the newly emerging gel layers toward the focal adhesions with the characteristic retrograde flow rate of 5 μm/min. The mathematical details are presented in Supporting Material A. The stress distributions are found numerically by means of COMSOL Multiphysics software (Numerical, Rishon Le-Zion, Israel). For the description of the physical model of the system, the rigorous definitions, and the details of calculations, see Supporting Material A.

RESULTS

Establishment and dynamics of the steady-state gel boundary

Infinite gel moving above one row of focal adhesions

The stress distribution in an infinite gel moving over a row of mature FAs located at a distance $L = 4$ μm from the leading edge with a separation $D = 4$ μm between the adjacent FAs is presented in Fig. 3 *a*. The stresses emerging within the gel are characterized by a distribution of the maximal local stress σ_1 (see Supporting Material A for definition) presented by the color code in Fig. 3 *a*. The regions around the focal adhesions and between them exhibit a positive (i.e., stretching) maximal stresses. The black lines in Fig. 3 *a* delimit the

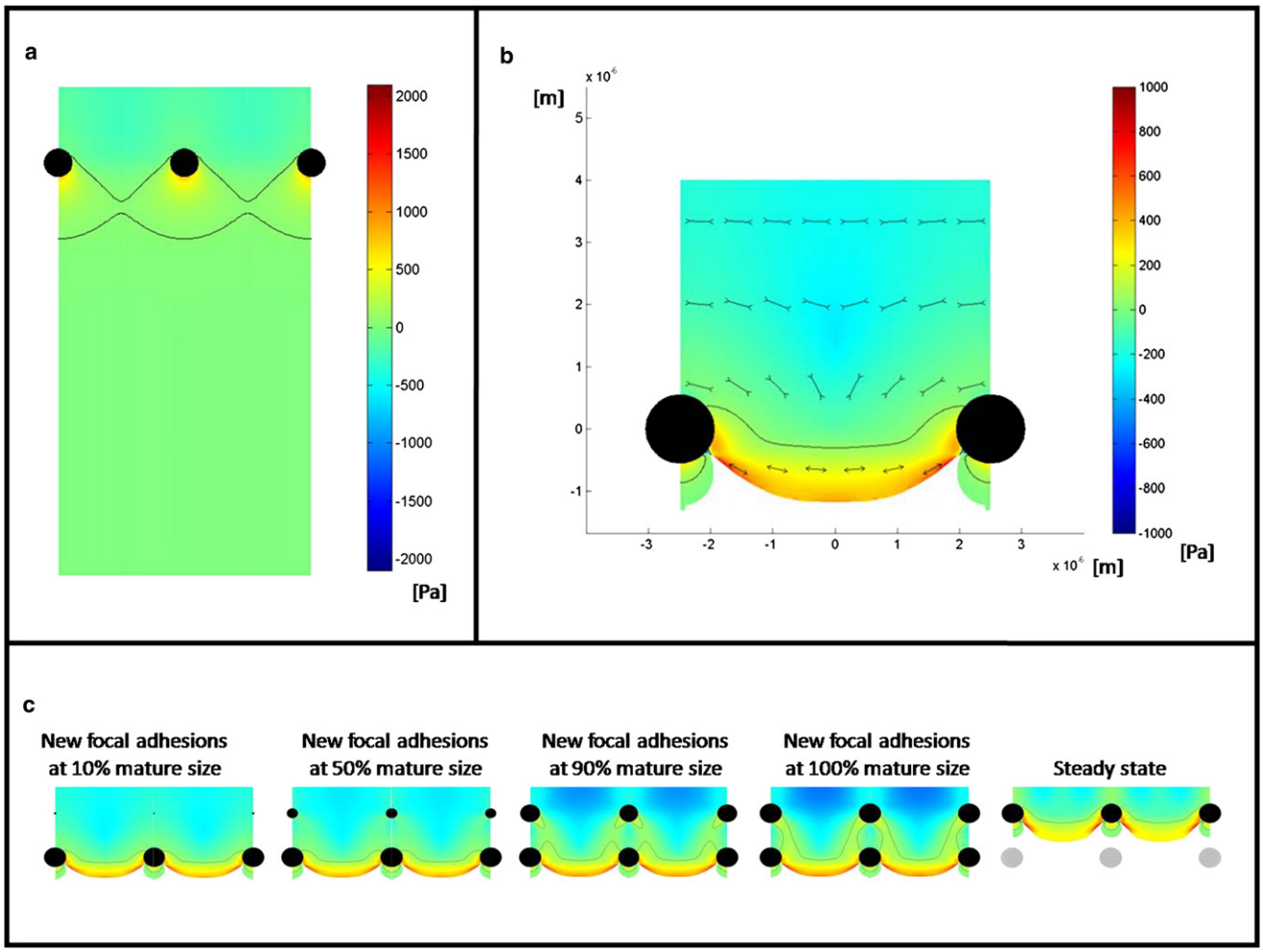

FIGURE 3 Formation and progression of the gel boundary. (*a*) Stress distribution before gel disintegration and generation of the zone of gel-disintegrating stresses. (*b*) The computed equilibrium gel boundary. The color bar determines the value of the maximal stress σ_1 in Pa. The lines with arrowheads and arrow tails indicate the stretching and compression stresses, respectively. The boundary of the region of the disintegration stress $\sigma_1 > \sigma_{th}$ is indicated by a black line. (*c*) Transition of the gel boundary as a result of growth of a new FA row. The new row of focal adhesions forms at the distance of 2 μm from the leading-edge membrane. Parameter values: $R_{FA} = 0.6$ μm, $D = 4$ μm, $L = 4$ μm, $f = 600$ Pa, and $\sigma_{th} = 40$ Pa.

region where the positive maximal stress σ_1 is larger than the threshold value $\sigma_{th} = 40$ Pa. According to our model, the region between the black lines has to disintegrate.

Establishment of the steady-state boundary of the gel

After disassembly of the gel region subjected to the gel-disintegrating stresses, $\sigma_1 > \sigma_{th}$, a break is formed across the whole length of the actin gel such that the break's upper boundary passes through the row of focal adhesions. Reestablishment of the equilibrium under new conditions is accompanied by adopting by the gel boundary of an equilibrium new shape.

We computed the equilibrium boundary shape and the corresponding distribution of the maximal stress σ_1, which are presented in Fig. 3 *b* with arrows indicating the lines of equal stress.

A concave steady-state shape of the gel boundary between the focal adhesions similar to that observed experimentally in Fig. 1 is achieved for specific values of the free parameters of the model (the threshold stress of disintegration, σ_{th}, and the friction force f). Fitting the calculated shapes of the gel boundary to the experimental shapes (Fig. 1 *c*) under requirements that f varies in the vicinity of 500 Pa, and that the gel thickness equals 200 nm, leads to $\sigma_{th} = 40$ Pa and $f = 600$ Pa. The fitting results are presented in Fig. 1 *c*.

Our computations predict the following scenario of the equilibrium boundary dynamics. Establishment of the equilibrium gel boundary results in creation in its vicinity of a new zone of gel-disintegrating stresses with the lines of equal stress parallel to the boundary profile (Fig. 3 *b*). At the same time, the gel keeps moving in the retrograde direction, resulting in retrograde progression of the equilibrium gel boundary and expansion of the zone of gel-disintegrating stresses. This movement lasts for a time τ_{rup}, after which the gel disintegrates instantaneously back to the line of threshold stress, $\sigma_1 = \sigma_{th}$, indicated by a black line in Fig. 3 *b*. This

disintegration brings the system out of the equilibrium again and must be followed by another cycle of reestablishment of an equilibrium gel boundary. As a result, the gel boundary undergoes cyclic leaps between the equilibrium and nonequilibrium shapes represented in Fig. 3 *b* by the boundary contour and the black line contour, respectively. The regime of a repeating cycle of boundary progression and backward leaping will be referred to as the steady-state regime, and the equilibrium boundary shape just before the leaping of the boundary back to the line $\sigma_1 = \sigma_{th}$ will be called the steady-state shape (Fig. 3 *b*).

It has to be emphasized that, on a qualitative level, the shape of the gel boundary, represented by a series of concave curves with the FAs at their intercepts, is largely insensitive to small changes of systems parameters. However, the subtle details of the boundary contour depend on the actual size, shape, and position of the FA, as well as on the velocity vector of the retrograde actin flow and the possible deviation of the leading edge from the straight shape.

Transition of the gel boundary to an emerging row of new FAs

Taking the steady-state boundary computed in the previous section as the initial state, we introduce a row of emerging focal adhesions growing halfway between the existing FA row and the leading edge membrane. The size of the new FAs is assumed to increase gradually up to the radius R_{FA} of the mature FAs within a time span denoted byτ_{FA}. We perform the calculation of stresses and strains within the gel and determine the shape of the gel boundary for a sequence of intermediate dimensions of the new FAs, their radius r changing in the range of $1/10\,R_{FA} \le r \le R_{FA}$. We look for the conditions where the new FAs generate a zone of gel-disintegrating stresses within the gel interior, and, hence, lead to formation of a new boundary, which is advanced, as compared to the previous one, toward the leading edge. The boundary transition is complete once the preexisting mature FAs get separated from the bulk of the gel. We assume the FA growth to be rapid as compared to the gel rupture, $\tau_{FA} << \tau_{rup}$, and the new focal adhesions to be oriented in line with the preexisting ones (Fig. 3 *c*).

As illustrated in Fig. 3 *c*, the growth of the new row of FAs produces a region of gel-disintegrating stresses that propagates, in the course of FA maturation, throughout the zone between the preexisting and the newly-maturating FAs. When the growing FAs achieve the fully mature size ($r = R_{FA}$), the upper boundary of the region of gel-disintegrating stresses is represented by a series of continuous lines connecting the new FAs. As a result, at the moment the initial rupture generation and the following disintegration of the gel occur, the new boundary forms along the new FA row, whereas the preexisting FAs remain outside of the actin gel. Thus, the lamellipodium interface progresses from the preexisting to the newly formed row of FAs. We investigated the boundary progression for other mutual positions of the preexisting and newly maturating FA rows and for a relatively slow rate of the FA growth and found, qualitatively, a similar behavior (data not shown).

Quantitative criteria for formation of the lamellipodium-lamellum interface

Our model indicates that the main parameters governing the formation of the lamellipodium-lamellum interface are: the size of the focal adhesions, R_{FA}; the spacing D between the individual FAs in the row; and the frictional force f per unit FA area. Using the fitted value for the threshold stress, $\sigma_{th} = 40$ Pa, we checked whether or not a continuous lamellipodium-lamellum interface forms, while varying the above parameters. The results are presented as phase diagrams in Fig. 4. The implications of these quantitative results are discussed in the following section.

PREDICTIONS AND IMPLICATIONS

Decrease of the FA-actin friction force can prevent formation of the lamellipodium-lamellum interface: implication for keratocytes

According to the model results illustrated in Fig. 4, *a–c*, substantial reduction of the friction force f can prevent the lamellipodium-lamellum interface formation for any FA size R_{FA} and any FA-FA separation D. Our model predicts that there is a minimal value of this force, $f_{min} = 270$ Pa, that is required for boundary formation, regardless of the values of other parameters. Smaller friction forces generate weak stretching stresses, which are insufficient for gel disintegration, and, hence for gel boundary formation.

The friction force per unit FA area f depends on the rate of the gel translocation with respect to the focal adhesions, the slower the rate the smaller the force f. Hence, the lamellipodium-lamellum interface formation must be directly related to the rate of the actin retrograde flow in the lamellipodium.

This outcome of the model explains the difference in actin organization between fast-crawling keratocytes and nonpolarized resting keratocytes (Fig. 5). The actin retrograde flow rate is expected to depend on the velocity of the leading edge progression; the larger the latter, the smaller the former. In the fast-crawling fish keratocytes, actin gel moves rather slowly (33), if at all (35,36), with respect to the substrate, and, hence, with respect to focal adhesions. In this case, the interaction between membrane and gel and the friction force between the FAs and actin should be minimal, resulting in small or even vanishing stresses within the gel. At the same time, resting keratocytes exhibit a considerable retrograde motion of actin with respect to the substrate, which must result in substantial FA-actin friction forces generating the stresses sufficient to drive the lamellipodium-lamellum interface formation. In accord with these predictions, whereas resting nonpolarized keratocytes exhibit a separation of the actin network into a well-defined lamellipodium and

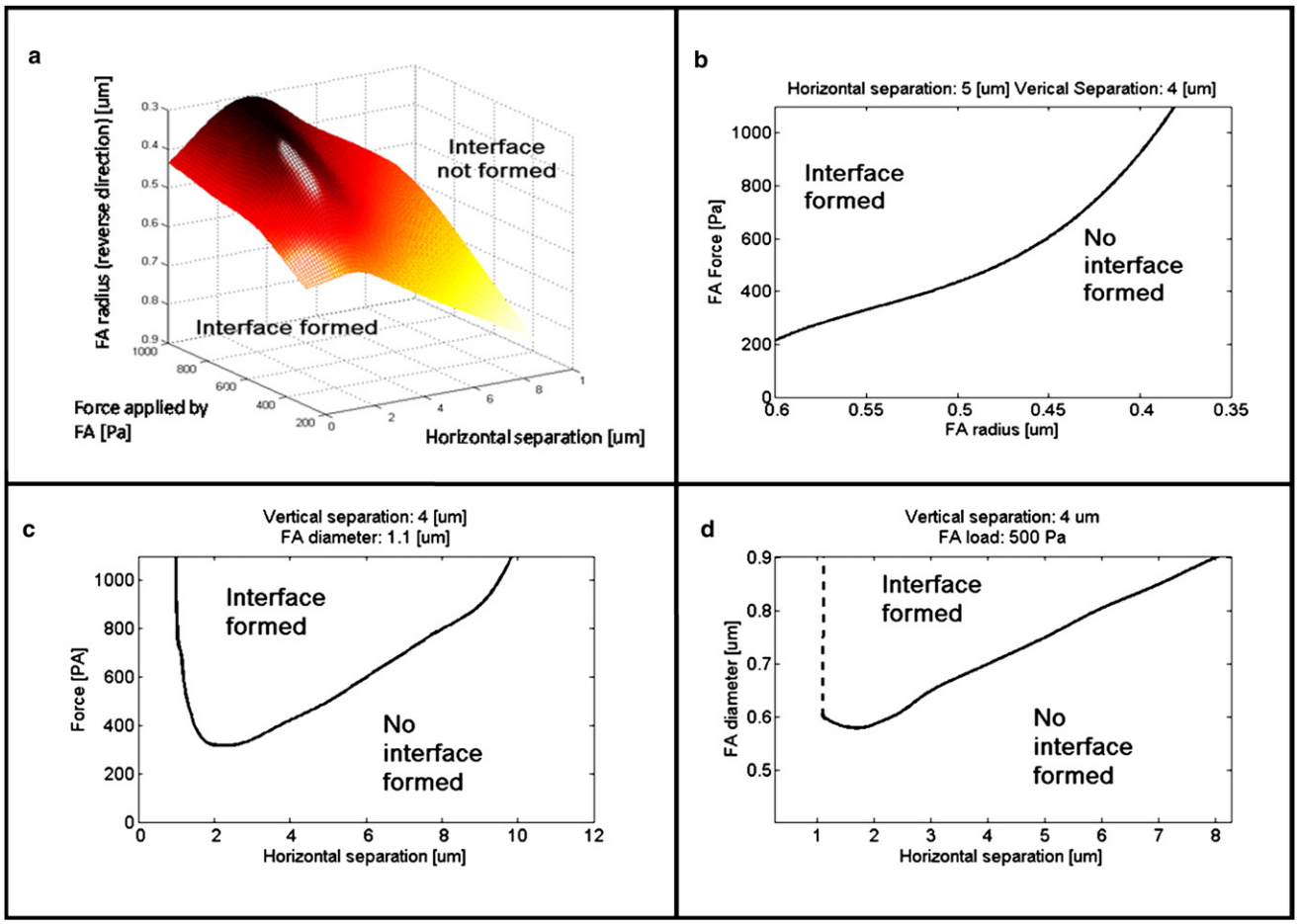

FIGURE 4 Phase diagrams representing criteria for formation of a lamellipodium-lamellum interface in terms of focal adhesion radius R_{FA}; distance between adhesions D, and friction force f per unit area of focal adhesion. (*a*) Three-parameter phase diagram. (*b*) Phase diagram for fixed $D = 5$ μm. (*c*) Phase diagram for fixed $R_{FA} = 0.55$ μm. (*d*) Phase diagram for fixed $f = 500$ Pa.

lamellum with a clear boundary between them (Fig. 5, *left panel*), in the crawling keratocytes the lamellipodium-lamellum interface does not form (Fig. 5, *right panel*).

Increase or decrease of the focal adhesion density prevents formation of the lamellipodium boundary

Our model predicts (Fig. 4, *a*, *c*, and *d*) that even if the friction force f per unit FA area and the FA radius R_{FA} allow, in principle, for formation of the lamellipodium-lamellum interface, this process can be prevented by an unsuitable focal adhesion density. If the row of the focal adhesions is too dense (small D) or too sparse (large D), a continuous region of disintegrations stretching stresses does not form, and hence, we predict that the boundary would not form.

Decrease of the focal adhesion size prevents formation of the lamellipodium-lamellum interface

According to the model results (Fig. 4, *a*, *b*, and *d*), if the individual FAs are too small, the stresses that develop within the lamellipodium gel are not sufficient to exceed the threshold value, and there will be no formation of a lamellum-lamellipodium interface. For every specific values of f and D, segregation of the actin gel into lamellipodium and lamellum is predicted to occur only if the FA radius exceeds a certain value given by the phase diagram (Fig. 4).

The focal adhesion area depends on the pulling force applied to the FA by the actin-myosin stress fibers ((37) and references therein). Hence, the myosin-mediated tension can regulate formation of the lamellipodium-lamellum interface through control of the FA size.

Formation of the lamellipodium-lamellum interface may contribute to generation of actin bundles within the lamellum

Lamellipodium and lamellum have differently organized actin networks. A distinct feature of the lamellum is the existence of two families of actin bundles: the first consists of the dorsal bundles (stress fibers) connected to the focal adhesions and stretching from the cell edge toward the cell center, and the second is composed of arclike bundles perpendicular

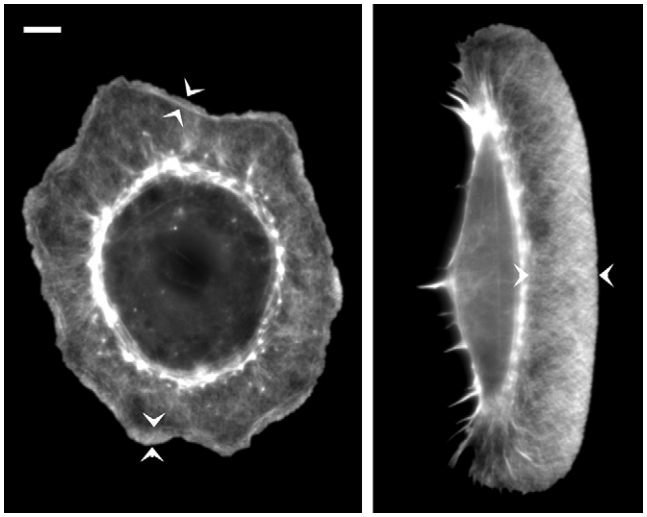

FIGURE 5 Fish epidermal keratocytes. (*Left panel*) Unpolarized resting cell with a fast retrograde movement of the actin gel with respect to the focal adhesions; arrowheads show the limits of the well-defined lamellipodia. (*Right panel*) Polarized fast crawling cell with very slow retrograde motion of the actin gel with respect to the substrate. No lamellipodium-lamellum interface forms. Bar, 5 μm.

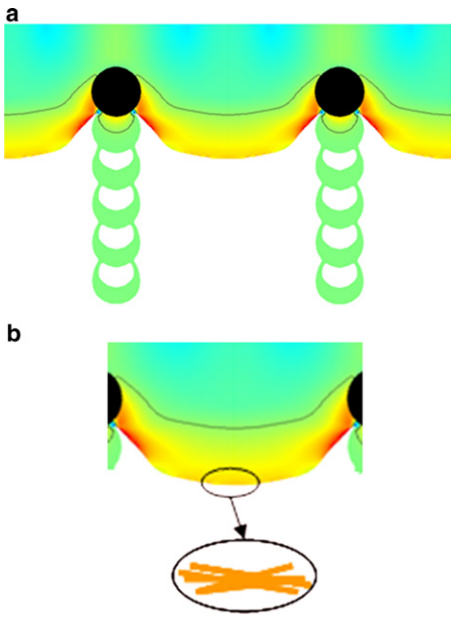

FIGURE 6 Hypothetical mechanisms of nucleation of actin bundles. (*a*) The actin tail of a focal adhesion as a remnant of the lamellipodial region of actin gel that did not undergo disintegration. (*b*) Nucleation of the arclike stress fibers.

to the dorsal bundles (19). Our computations predict that the origin of the dorsal bundles can be related to the structure of the actin gel in the shadow of focal adhesions, i.e., right behind them. According to our results, the character of the stress distribution in these regions is different from that between the FAs. The area of the gel-disintegrating stresses in the shadow of every FA is small and surrounded by the region where no disintegration occurs. As a result, our model predicts formation of a chainlike actin tail growing after each FA location toward the cell center (Fig. 6 *a*). The elements of such a chain correspond to portions of the gel, which pass above the FA and do not undergo disintegration. The width of the emerging actin tail is close to the FA diameter. It has to be noted that the shape and conformation of the actin tail are sensitive to the form of the FAs. The computations for elliptic rather than circular focal adhesions (not shown) demonstrated no gel-disintegrating regions within the tail element and a smoother shape of the tail itself. Since the tail protrudes outside the lamellipodium, its characterization is not considered by this model, which suggests only a mechanism of nucleation of the tail formation behind the FAs. Even though the evolution of the actin tail into a stress fiber is out of the scope of our model, we believe that it requires an additional qualitative switch in the composition. In particular, the Arp2/3 complexes have to leave and get replaced, probably, by another type of nucleator of actin polymerization represented, perhaps, by formins (19). A key event of transition from the stress fiber precursors to the mature stress fibers must be bundling of actin filaments mediated by α-actinin and myosin IIA (34). Further evolution of the stress fiber-FA complex strongly depends on the mechanical forces developed due to the acto-myosin contractility (37,38). The mechanism of this mechanosensitivity may involve a force-dependent recruitment of some specialized proteins such as zyxin (39,40).

The arclike stress fibers appear to assemble by end-to-end annealing of short Arp2/3-containing actin bundles generated in the lamellipodium (19). According to our model, the reason for formation of these short actin bundles may be related to the distribution of stresses next to the lamellipodium boundary in its equilibrium state. As discussed above, these stresses are positive, i.e., they correspond to gel stretching, are directed tangentially to the boundary, and reach values of hundreds of Pascal next to the boundary (Fig. 3 *b*). Such stresses must generate considerable polarization of the actin filaments within the gel such that the average filament orientation also becomes parallel to the lamellipodium boundary. This may facilitate binding of actin-bundling proteins and myosin II and formation of bundlelike structures along the lamellipodium boundary (Fig. 1 *b*, *lower arrowhead*). If the mechanism of gel disintegration next to the boundary consists, at least partially, in decay of the network into pieces, the resulting separate gel elements can represent short actin bundles serving as building blocks of the arclike stress fibers. This can be facilitated by a suitable filament polarization and orientation within the cytoplasm.

DISCUSSION

We presented a physical mechanism by which focal adhesions can generate a boundary of the lamellipodium actin

network, hence, driving formation of a lamellipodium-lamellum interface.

Although, in general, formation of two actin networks in the cell edge can be recovered by numerical simulations of a combination of chemical reaction kinetics, G-actin diffusion, and actin filament transport (41), the specific geometric and dynamic features of the lamellipodium-lamellum interface observed experimentally (13) require consideration of other physical mechanisms with an essential role played by the focal adhesion-actin network interactions.

The mechanism we suggest is based on the established view of the lamellipodium in which the actin gel polymerizing next to the membrane at the cell leading edge moves in the retrograde direction toward the cell center and experiences a frictionlike interaction with focal adhesions immobilized on the extracellular substrate. At the heart of our model lies the assumption that the positive, stretching stresses generated within the actin network produce partial disintegration of the actin gel. Based on the representation of the actin gel as an isotropic elastic continuum (22), we computed the distribution of the stresses within the gel and found that, whereas the stresses are negative (compressing) in the major part of the gel, they become positive (stretching) in the vicinity of the focal adhesions and between them. Disintegration of the actin gel driven by these stresses generates the gel boundary associated with the focal adhesions.

Our model explains the formation of a distinct lamellipodium-lamellum interface demarcated by mature focal adhesions, reproduces the experimentally observed character of this interface consisting of a series of concave curves that have FAs at their connecting vertices, and treats the transition of the interface from the preexisting to the newly forming rows of focal adhesions.

Although the predicted and observed shapes of the interface are very similar, they are not precisely identical (Fig. 1 *c*). This may be expected due to deviations of the actual conditions within a cell from the model assumptions such as ideally symmetrical form of FAs, equal distance between FAs in a row, and a uniformly straight shape of the cell leading edge. Nevertheless, the computed theoretical interface closely matches the experimentally observed lamellipodium-lamellum interface (Fig. 1 *c*).

The model describes successfully the lamellipodium-lamellum interface forming within gel-like actin systems such as those of regular fibroblasts or epithelial cells (7,13,42) as well as mammalian or avian growth cones (see, e.g., (43)). At the same time, the model is not applicable to substantially different actin systems such as that of Aplysia growth cones whose prominent feature is a very high density of filopodia with adhesions at their tips (see, e.g., (44,45)).

It must be noted that, since the most essential element of the model is the friction forces between the actin gel and the focal adhesions, the lamellipodium-lamellum interface formation according to the same mechanism will occur if the retrograde motion of the actin gel is driven by the action of myosin (46) in addition to, or instead of, the actin polymerization at the leading edge.

We addressed the mechanism of advancing of the lamellipodium-lamellum interface driven by maturation of a new row of focal adhesions within the lamellipodium. We have found that propagation of the interface from the preexisting row of FAs to the newly maturating ones is not a continuous process, but rather is achieved through leaps that take place only when the size of the new FAs reaches a nearly full size of a mature FA.

Main assumption of the model

The crucial assumption of this model is that the lamellipodium actin gel gets disintegrated upon sufficiently large stretching stresses. This is analogous to the proposal underlying the suggested mechanism of the actin-based intracellular movement of some bacteria (25) and movement of beads coated with WASP VCA domain in a motility medium in vitro (26). We suggest that the stretching stresses developed within the actin network promote actin filaments severing by such proteins as ADF/cofilin and, perhaps, gelsolin.

The proteins of ADF/cofilin family are expressed by all types of cells and are critical for regulating actin cytoskeleton dynamics ((27) and references therein). Several mechanisms of biochemical regulation of the ADF/cofilin activity have been established ((27) and references therein). We suggest the stretching stress as another, mechanical, means of regulation of the ADF/cofilin activity and an additional contribution to the forces driving the actin filament severing. The stretching stress must be a universal severing factor complementary to biochemical regulators. Indeed, filament breakage is accompanied by a complete relaxation of the preexisting stretching stresses and release of the related elastic energy. Such energy discharge increases both the probability and the rate of the severing process. The disintegration is proposed to occur in the region adjacent to the lamellipodium boundary where the gel is subject to stretching stresses, varying in the range between about several hundred (up to 700 Pa) and several tens (down to 40 Pa) of Pascal. The lower stress limit of 40 Pa corresponds to the fitted value of the threshold stress σ_{th}.

There are different options for the actin network fate after its severing at the lamellipodium-lamellum interface. One possibility is a rapid depolymerization such as that produced by coaction of cofilin, coronin, and Aip1 (47). Another possibility is a rupture of the gel into pieces that serve as building blocks for the arclike actin bundles within the lamellum. Different modes of gel breakdown are not mutually exclusive and can proceed in parallel. At this stage, we do not elaborate on the detailed mechanism of the gel disintegration upon stretching stress, which requires separate experimental work and theoretical modeling.

SUPPORTING MATERIAL

A movie and additional equations are available at http://www.biophysj.org/biophysj/supplemental/S0006-3495(09)01269-7. The movie was also published as supplementary information to Alexandrova et al. (13).

We are grateful to Alex Mogilner and Anders Carlsson for helpful discussions.

Financial support for M.M.K. by the Israel Science Foundation and the Marie Curie Network "Flippases" is gratefully acknowledged. A.D.B. holds the Joseph Moss Professorial Chair in Biomedical Research and acknowledges support from the Minerva Foundation and the Maurice Janin fund.

REFERENCES

1. Ridley, A. J., M. A. Schwartz, K. Burridge, R. A. Firtel, M. H. Ginsberg, et al. 2003. Cell migration: integrating signals from front to back. *Science*. 302:1704–1709.
2. Lock, J. G., B. Wehrle-Haller, and S. Stromblad. 2008. Cell-matrix adhesion complexes: master control machinery of cell migration. *Semin. Cancer Biol.* 18:65–76.
3. Mogilner, A., and G. Oster. 1996. Cell motility driven by actin polymerization. *Biophys. J.* 71:3030–3045.
4. Mogilner, A., and G. Oster. 2003. Polymer motors: pushing out the front and pulling up the back. *Curr. Biol.* 13:R721–R733.
5. Salmon, W. C., M. C. Adams, and C. M. Waterman-Storer. 2002. Dual-wavelength fluorescent speckle microscopy reveals coupling of microtubule and actin movements in migrating cells. *J. Cell Biol.* 158:31–37.
6. Abercrombie, M., G. A. Dunn, and J. P. Heath. 1977. The shape and movement of fibroblasts in culture. *Soc. Gen. Physiol. Ser.* 32:57–70.
7. Ponti, A., M. Machacek, S. L. Gupton, C. M. Waterman-Storer, and G. Danuser. 2004. Two distinct actin networks drive the protrusion of migrating cells. *Science*. 305:1782–1786.
8. Vallotton, P., S. L. Gupton, C. M. Waterman-Storer, and G. Danuser. 2004. Simultaneous mapping of filamentous actin flow and turnover in migrating cells by quantitative fluorescent speckle microscopy. *Proc. Natl. Acad. Sci. USA*. 101:9660–9665.
9. Svitkina, T. M., and G. G. Borisy. 1999. Arp2/3 complex and actin depolymerizing factor/cofilin in dendritic organization and treadmilling of actin filament array in lamellipodia. *J. Cell Biol.* 145:1009–1026.
10. Lin, C. H., and P. Forscher. 1995. Growth cone advance is inversely proportional to retrograde F-actin flow. *Neuron*. 14:763–771.
11. Theriot, J. A., and T. J. Mitchison. 1992. Comparison of actin and cell surface dynamics in motile fibroblasts. *J. Cell Biol.* 119:367–377.
12. Cramer, L. P. 1997. Molecular mechanism of actin-dependent retrograde flow in lamellipodia of motile cells. *Front. Biosci.* 2:d260–d270.
13. Alexandrova, A. Y., K. Arnold, S. Schaub, J. M. Vasiliev, J. J. Meister, et al. 2008. Comparative dynamics of retrograde actin flow and focal adhesions: formation of nascent adhesions triggers transition from fast to slow flow. *PLoS One*. 3:e3234.
14. Borisy, G. G., and T. M. Svitkina. 2000. Actin machinery: pushing the envelope. *Curr. Opin. Cell Biol.* 12:104–112.
15. Pollard, T. D. 2004. Molecular mechanisms regulating actin filament dynamics at the leading edge of motile cells. *In* Cell Motility. A. Ridley, M. Peckham, and P. Clark, editors. Wiley, New York. 1–17.
16. Pollard, T. D., and G. G. Borisy. 2003. Cellular motility driven by assembly and disassembly of actin filaments. *Cell*. 112:453–465.
17. Gardel, M. L., B. Sabass, L. Ji, G. Danuser, U. S. Schwarz, et al. 2008. Traction stress in focal adhesions correlates biphasically with actin retrograde flow speed. *J. Cell Biol.* 183:999–1005.
18. Svitkina, T. M., A. A. Shevelev, A. D. Bershadsky, and V. I. Gelfand. 1984. Cytoskeleton of mouse embryo fibroblasts. Electron microscopy of platinum replicas. *Eur. J. Cell Biol.* 34:64–74.
19. Hotulainen, P., and P. Lappalainen. 2006. Stress fibers are generated by two distinct actin assembly mechanisms in motile cells. *J. Cell Biol.* 173:383–394.
20. Cai, Y., N. Biais, G. Giannone, M. Tanase, G. Jiang, et al. 2006. Nonmuscle myosin IIA-dependent force inhibits cell spreading and drives F-actin flow. *Biophys. J.* 91:3907–3920.
21. Zhang, X., G. Jiang, Y. Cai, S. J. Monkley, D. R. Critchley, et al. 2008. Talin depletion reveals independence of initial cell spreading from integrin activation and traction. *Nat. Cell Biol.* 10:1062–1068.
22. Ji, L., J. Lim, and G. Danuser. 2008. Fluctuations of intracellular forces during cell protrusion. *Nat. Cell Biol.* 10:1393–1400.
23. Wang, Y. L. 2007. Flux at focal adhesions: slippage clutch, mechanical gauge, or signal depot. *Sci. STKE*. 2007:pe10.
24. Hu, K., L. Ji, K. T. Applegate, G. Danuser, and C. M. Waterman-Storer. 2007. Differential transmission of actin motion within focal adhesions. *Science*. 315:111–115.
25. Sekimoto, K., J. Prost, F. Julicher, H. Boukellal, and A. Bernheim-Grosswasser. 2004. Role of tensile stress in actin gels and a symmetry-breaking instability. *Eur. Phys. J. E Soft Matter*. 13:247–259.
26. Bernheim-Groswasser, A., S. Wiesner, R. M. Golsteyn, M. F. Carlier, and C. Sykes. 2002. The dynamics of actin-based motility depend on surface parameters. *Nature*. 417:308–311.
27. Bamburg, J. R., and B. W. Bernstein. 2008. ADF/cofilin. *Curr. Biol.* 18:R273–R275.
28. Andrianantoandro, E., and T. D. Pollard. 2006. Mechanism of actin filament turnover by severing and nucleation at different concentrations of ADF/cofilin. *Mol. Cell*. 24:13–23.
29. Galkin, V. E., A. Orlova, M. S. VanLoock, A. Shvetsov, E. Reisler, et al. 2003. ADF/cofilin uses an intrinsic mode of F-actin instability to disrupt actin filaments. *J. Cell Biol.* 163:1057–1066.
30. Ono, S. 2007. Mechanism of depolymerization and severing of actin filaments and its significance in cytoskeletal dynamics. *Int. Rev. Cytol.* 258:1–82.
31. Paavilainen, V. O., E. Oksanen, A. Goldman, and P. Lappalainen. 2008. Structure of the actin-depolymerizing factor homology domain in complex with actin. *J. Cell Biol.* 182:51–59.
32. Wang, W., R. Eddy, and J. Condeelis. 2007. The cofilin pathway in breast cancer invasion and metastasis. *Nat. Rev. Cancer*. 7:429–440.
33. Vallotton, P., G. Danuser, S. Bohnet, J. J. Meister, and A. B. Verkhovsky. 2005. Tracking retrograde flow in keratocytes: news from the front. *Mol. Biol. Cell*. 16:1223–1231.
34. Choi, C. K., M. Vicente-Manzanares, J. Zareno, L. A. Whitmore, A. Mogilner, et al. 2008. Actin and α-actinin orchestrate the assembly and maturation of nascent adhesions in a myosin II motor-independent manner. *Nat. Cell Biol.* 10:1039–1050.
35. Theriot, J. A., and T. J. Mitchison. 1991. Actin microfilament dynamics in locomoting cells. *Nature*. 352:126–131.
36. Svitkina, T. M., A. B. Verkhovsky, K. M. McQuade, and G. G. Borisy. 1997. Analysis of the actin-myosin II system in fish epidermal keratocytes: mechanism of cell body translocation. *J. Cell Biol.* 139:397–415.
37. Bershadsky, A., M. Kozlov, and B. Geiger. 2006. Adhesion-mediated mechanosensitivity: a time to experiment, and a time to theorize. *Curr. Opin. Cell Biol.* 18:472–481.
38. Riveline, D., E. Zamir, N. Q. Balaban, U. S. Schwarz, T. Ishizaki, et al. 2001. Focal contacts as mechanosensors: externally applied local mechanical force induces growth of focal contacts by an mDia1-dependent and ROCK-independent mechanism. *J. Cell Biol.* 153:1175–1186.
39. Colombelli, J., A. Besser, H. Kress, E. G. Reynaud, P. Girard, et al. 2009. Mechanosensing in actin stress fibers revealed by a close correlation between force and protein localization. *J. Cell Sci.* In press.
40. Zaidel-Bar, R., M. Cohen, L. Addadi, and B. Geiger. 2004. Hierarchical assembly of cell-matrix adhesion complexes. *Biochem. Soc. Trans.* 32:416–420.

41. Huber, F., J. Kas, and B. Stuhrmann. 2008. Growing actin networks form lamellipodium and lamellum by self-assembly. *Biophys. J.* 95:5508–5523.

42. Abraham, V. C., V. Krishnamurthi, D. L. Taylor, and F. Lanni. 1999. The actin-based nanomachine at the leading edge of migrating cells. *Biophys. J.* 77:1721–1732.

43. Mongiu, A. K., E. L. Weitzke, O. Y. Chaga, and G. G. Borisy. 2007. Kinetic-structural analysis of neuronal growth cone veil motility. *J. Cell Sci.* 120:1113–1125.

44. Burnette, D. T., L. Ji, A. W. Schaefer, N. A. Medeiros, G. Danuser, et al. 2008. Myosin II activity facilitates microtubule bundling in the neuronal growth cone neck. *Dev. Cell.* 15:163–169.

45. Zhang, X. F., A. W. Schaefer, D. T. Burnette, V. T. Schoonderwoert, and P. Forscher. 2003. Rho-dependent contractile responses in the neuronal growth cone are independent of classical peripheral retrograde actin flow. *Neuron.* 40:931–944.

46. Giannone, G., B. J. Dubin-Thaler, O. Rossier, Y. Cai, O. Chaga, et al. 2007. Lamellipodial actin mechanically links myosin activity with adhesion-site formation. *Cell.* 128:561–575.

47. Kueh, H. Y., G. T. Charras, T. J. Mitchison, and W. M. Brieher. 2008. Actin disassembly by cofilin, coronin, and Aip1 occurs in bursts and is inhibited by barbed-end cappers. *J. Cell Biol.* 182:341–353.